

PAPER • OPEN ACCESS

Experimental study on tool wear of side cutting edge in micro-milling

To cite this article: X M Yang *et al* 2019 *IOP Conf. Ser.: Mater. Sci. Eng.* **504** 012102

View the [article online](#) for updates and enhancements.

Experimental study on tool wear of side cutting edge in micro-milling

X M Yang, X Cheng^{*}, F Wang, Q L Sun and W H Wang

Shandong University of Technology, Zibo, 255049, China

Corresponding author and e-mail: X Cheng, chengxsdut@163.com

Abstract. Micro-milling technology is becoming more and more essential in many fields in which the miniature parts are widely applied. Research of tool wear occupies an important part in micro-milling studies. In this paper, the micro end mills of 1 mm in diameter with coating TiAlN are used to conduct micro-milling parameters studies on tool wear of side cutting edge for brass H59. The wear form and wear mechanism of tools are analyzed firstly. The wear forms include coating peeling, the rounding of corner radius and cutting edge chipping, and the wear mechanisms include abrasive wear and adhesive wear. Orthogonal experiments are carried out to obtain significance order of key parameters for the wear band width of side cutting edge and the optimal parameters combination. The orthogonal experiments results show that the significance order of key parameters for wear band width from large to small is feed engagement f_z , axial depth of cut a_p , spindle speed n and radial depth of cut a_e . The optimal parameters combination obtained is $f_z = 2 \mu\text{m/z}$, $a_p = 0.3 \text{ mm}$, $n = 60000 \text{ min}^{-1}$, $a_e = 0.15 \text{ mm}$. The study provides a valuable reference for the selection of milling parameters to reduce tool wear in actual machining.

1. Introduction

Many fields ranging from bio-medical devices to defense applications are widely using parts and devices with micron-scale characteristic dimensions [1]. Over the last few years conventional devices have tremendously grown in the complexity of their functions and levels of performance which has directly impacted their manufacturing accuracy, whereas it is not enough. It has become an inevitable choice to develop micromachining technology, which has the advantages of small force on workpiece, high machining precision, wide processing range and superior processing performance [2]. Micro-milling is one of micromachining technology. The diameter of the milling cutter used in micro-milling is equal to or smaller than 1 mm [3]. However, with the miniaturization of cutting tools and high cutting speed, tool wear is rapid in micro-milling process. This not only reduces the tool life and increases the processing cost, but also reduces the machining accuracy and limits the development of micro-milling. Therefore, it is of great significance to study the tool wear in micro-milling.

Kuram has studied the effects of spindle speed, feed per tooth and depth of cut on tool wear during micro-milling of aluminum using Taguchi experimental design method. It has showed that tool wear increased with spindle speed and depth of cut [4]. Zhu have introduced a novel approach for TCM in micro-milling. The tool state can be estimated by shape variations of the cutting force wave forms [5]. Saedon has presented the findings of an experimental investigation of the effect of cutting speed, feed per tooth and depth of cut on tool life and material removal in micro-milling of AISI D2 steel using



TiAlN coated tool. It has showed that higher cutting speed imposes higher cutting force over cutting edges and higher stress especially as intermittence cutting process thus suddenly chipping the cutting edges, which ultimately reduce the micro tool diameter thus shorten the tool life [6]. Biermann et al have conducted the investigation of different hard coatings for micro-milling of austenitic stainless steel 304. They have found that the application of a TiAlN and AlCrN coating generated very good results regarding the tool wear [7]. Thepsonthi has used a finite element based modeling of micro milling and has calculated the optimized tool path and milling conditions for micromachining of titanium alloy Ti6AL4V by considering surface roughness and burr formation. They concluded that tool path strongly affects tool wear [8]. Popov has investigated the influence of feed rate on tool wear, and they observed that each too experiences a different amount of wear during machining. They proposed a tool wear term defining the average increase in cutting edge radius [9]. Oliaei has conducted investigation to understand the relationship between milling process parameters (radial depth of cut and feed per tooth) and tool wear during circular pocket micro milling of Stavax with tungsten carbide micro end mills. The results have showed that radial depth of cut and feed per tooth values must be selected in conjunction during the process planning stage of pocket micro-milling, and 60 % radial depth of cut yielded better tool performance compared to lower and higher radial depth of cut values [10]. Cheng has introduced a new method to build a general model for estimating the critical micro-milling conditions for single crystalline silicon by considering micro-milling process variables based on the generally-accepted indentation model. The analytical results show that cutting edge radius and the feed rate affect the critical conditions greatly [11].

As above, many scholars have studied tool wear and the researches mainly focus on the flank face of bottom edge and corner radius. The relationship between spindle speed, feed per tooth, axial cutting depth, radial depth of cut and tool wear is less studied. In this paper, the orthogonal test method is adopted to conduct the parameter experiments of tool wear of side cutting edge in micro-milling brass H59. The wear band width of side cutting edge is experiment index, and the key parameters (spindle speed, feed per tooth, axial depth of cut, radial depth of cut) are set as experiment factors. The significance sequence of four milling parameters on tool wear is obtained by analyzing the experiments results. Meanwhile, the wear form and mechanism analysis of tool wear are carried out.

2. Experiment set-up

A novel miniaturized three-axis micro-milling machine tool 3A-S100 is used in micro-milling experiments as shown in Figure 1. Three motion axes of the machine tool are driven by linear motors and motion resolution of each axis is 0.1 μm . The travel of the machine tool is 100 mm. The axial float and radial runout are less than 1 μm [12]. The machine spindle is the electric spindle which speed is adjustable, and the highest speed is 80,000 min^{-1} .



Figure 1. Machine tool 3A-S100.

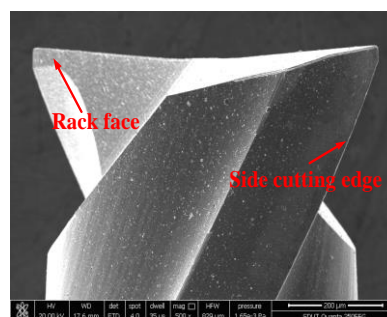


Figure 2. New micro end mill.

In the micro-milling experiments, TiAlN coated two-flute cemented carbide end mills with a diameter of 1mm are employed. The helix angle of the tools is 30°. A new cutting tool is used for each experiment. Before cutting experiments, each cutter is imaged by using scanning electron microscope

(SEM) to ensure that the tool surface is free of defects as shown in Figure 2. Brass H59 is chosen as workpiece material and the dimension of workpieces is $10 \times 10 \times 10$ mm, the chemical composition of the material as shown in Table 1. Before experiments, the workpiece samples are pre-milled to eliminate any surface defects and to provide flatness.

Table 1. The chemical composition of brass H59.

| Element | Cu | Zn | Pb | Fe | Sb | P |
|------------|-------|-------|------|------|-------|-------|
| Weight (%) | 57~60 | 40~43 | <0.5 | <0.3 | <0.01 | <0.01 |

In orthogonal experiments, the experimental factors include spindle speed, feed per tooth, axial depth of cut and radial depth of cut, and the wear band width of side cutting edge is the experiment index. The milling length of each experiment group is 200m according to previous experiments study. After micro-milling experiments, the tools are measured by SEM. The wear band widths refer to the distance from the outside edge profile to the boundary of the wear area. The widths are measured from 6 different sites and then averaged. The mean of wear band width is used to assess the tool wear.

The factors and levels of the experiments are shown in Table 2. The L_{16} orthogonal table is designed without considering the influence between the factors.

Table 2. The factors and levels of the experiments.

| No. | a_e (mm) | a_p (mm) | f_z ($\mu\text{m}/\text{z}$) | n (min^{-1}) |
|-----|---------------|---------------|-------------------------------------|------------------------------|
| 1 | 0.10 | 0.25 | 1.5 | 40000 |
| 2 | 0.15 | 0.30 | 2.0 | 50000 |
| 3 | 0.20 | 0.35 | 2.5 | 60000 |
| 4 | 0.25 | 0.40 | 3.0 | 70000 |

3. Results and discussion

3.1. Wear form and wear mechanism

As the high-temperature chip flows through the rake face, and the thermal expansion coefficient of the tool substrate is different from that of the coating material, the temperature in the contact area between the tool and the workpiece frequently changes. The tool body material exposes as shown in Figure 3. Due to the tip is subjected to extrusion, shear, friction and impact, and the coating strength at the tip is weaker than that at other parts. The corner radius of the tip becomes larger with the increasement of cutting time. Due to the uneven impact on the side edge when it is cut in and out, the stress distribution on the cutting edge changes constantly, and cutting edge chipping phenomenon has occurred as shown in Figure 4.

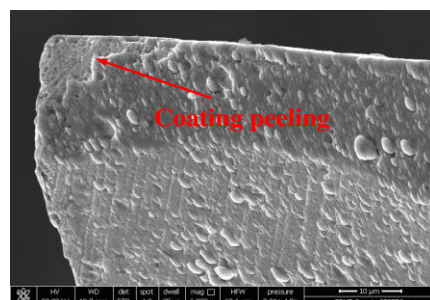


Figure 3. Coating peeling.

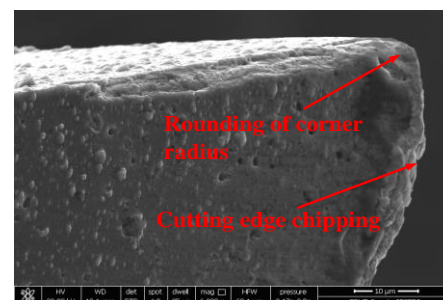


Figure 4. The rounding of corner radius and cutting edge chipping.

The abrasive wear is to form when the carbides and oxide hard spots in the workpiece material to rub and scribe workpieces surface. FeC hard spots more easily generate since brass H59 contains Fe element as shown in Table 1. These hard spots rub between the workpiece and the tool, which easily cause the tool material to fall off and form scratches, as shown in Figure 5.

The friction action between the tool and the workpiece produce the adhesive wear under the action of high temperature and high pressure. Then the plastic deformation and the cold welding phenomenon occur. When the two are in relative motion, the adhesive particles of material are taken away to form adhesive wear. Generally speaking, the fracture of the bonding point occurs on the lower hardness side, which is the workpiece material. However, there is microscopic unevenness on the surface of the tool, and the internal stress is often uneven in the structure. Therefore, the tool surface coating is often broken and taken away by the workpiece material, which results in the tool wear.

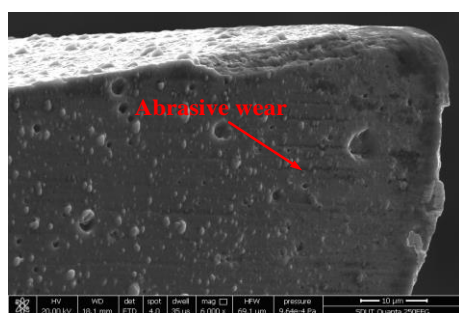


Figure 5. Abrasive wear at flank face.

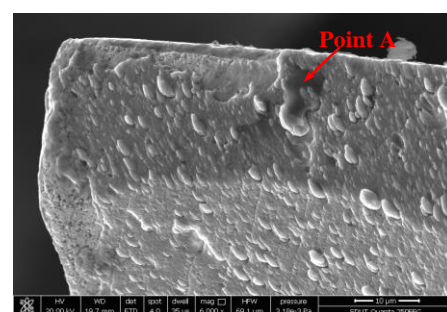


Figure 6. Adhesive wear at rake face.

Under the action of high temperature and high pressure, the cutting chip of workpiece adheres to the tool surface to form a chip accumulation tumor and the coating material of the tool are taken away in the process of micromilling brass. The adhesive substance appeared at the rake face as shown in Figure 6. In order to determine the composition of the adhesive substance, the energy spectrum analysis is performed on point A as shown in Figure 7. For comparison, the energy analysis of the coating of new tool is performed as shown in Figure 8. Compared with the coating composition of the new tool, the contents of Cu and Zn in point A are very high. It confirms that the adhesive substance is brass. It also proves that the wear mechanism is the adhesive wear.

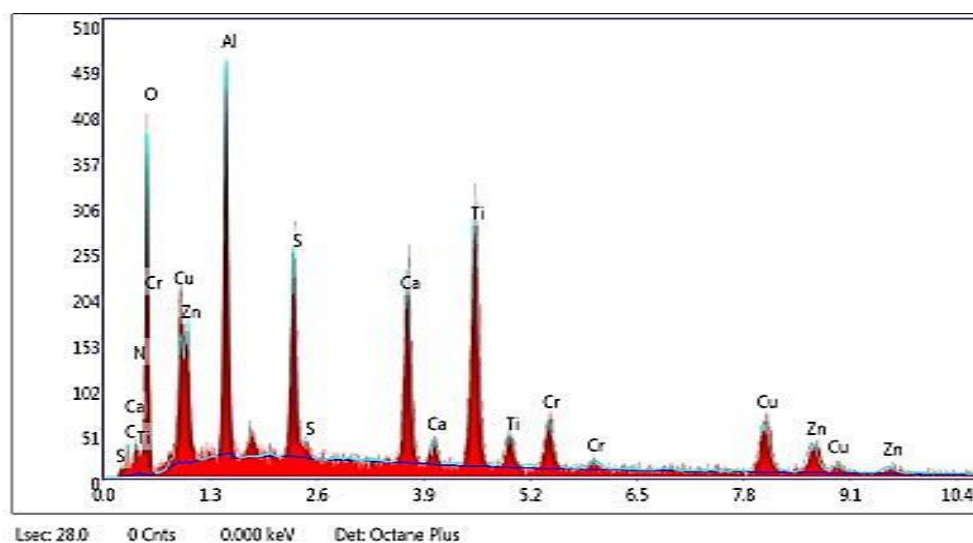


Figure 7. Gamma spectrum of bonding coat at point A.

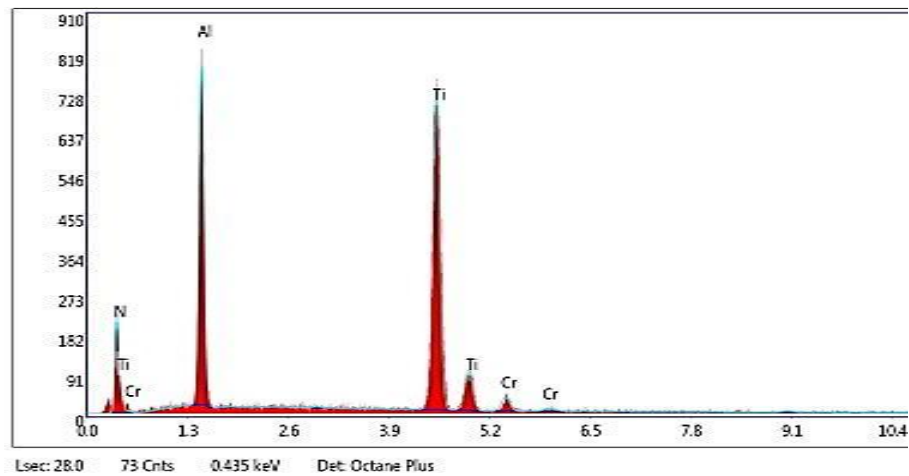


Figure 8. Gamma spectrum of a new milling cutter.

In summary, when micro-milling brass material, the main wear forms of the tool include coating peeling, the rounding of corner radius and cutting edge chipping. The wear mechanisms include abrasive wear and adhesive wear by above analyses.

3.2. Orthogonal optimization experiment results

The orthogonal experiments design and its results are shown in Table 3.

Table 3. Orthogonal experiments table.

| No. | a_e (mm) | a_p (mm) | f_z ($\mu\text{m}/\text{z}$) | n (min^{-1}) | Wear band width(μm) |
|------------------|--|------------|----------------------------------|---------------------------|----------------------------------|
| 1 | 0.10 | 0.25 | 1.5 | 40000 | 4.03 |
| 2 | 0.10 | 0.30 | 2.0 | 50000 | 2.88 |
| 3 | 0.10 | 0.35 | 2.5 | 60000 | 4.93 |
| 4 | 0.10 | 0.40 | 3.0 | 70000 | 5.57 |
| 5 | 0.15 | 0.25 | 2.0 | 60000 | 3.99 |
| 6 | 0.15 | 0.30 | 1.5 | 70000 | 4.42 |
| 7 | 0.15 | 0.35 | 3.0 | 40000 | 5.33 |
| 8 | 0.15 | 0.40 | 2.5 | 50000 | 3.38 |
| 9 | 0.20 | 0.25 | 2.5 | 70000 | 4.13 |
| 10 | 0.20 | 0.30 | 3.0 | 60000 | 4.44 |
| 11 | 0.20 | 0.35 | 1.5 | 50000 | 5.82 |
| 12 | 0.20 | 0.40 | 2.0 | 40000 | 5.30 |
| 13 | 0.25 | 0.25 | 3.0 | 50000 | 5.38 |
| 14 | 0.25 | 0.30 | 2.5 | 40000 | 5.32 |
| 15 | 0.25 | 0.35 | 2.0 | 70000 | 4.53 |
| 16 | 0.25 | 0.40 | 1.5 | 60000 | 3.78 |
| K_1 | 17.400 | 17.515 | 18.030 | 19.965 | |
| K_2 | 17.110 | 17.040 | 16.685 | 17.440 | |
| K_3 | 19.670 | 20.600 | 17.745 | 17.130 | |
| K_4 | 18.990 | 18.015 | 20.710 | 18.635 | |
| k_1 | 4.3500 | 4.3788 | 4.5075 | 4.9913 | |
| k_2 | 4.2775 | 4.2600 | 4.1713 | 4.3600 | |
| k_3 | 4.9175 | 5.1500 | 4.4363 | 4.2825 | |
| k_4 | 4.7475 | 4.5038 | 5.1775 | 4.6588 | |
| Range | 0.6400 | 0.8900 | 1.0063 | 0.7088 | |
| factors | $f_z > a_p > n > a_e$ | | | | |
| Optimal solution | $f_z = 2 \mu\text{m}/\text{z}$, $a_p = 0.3 \text{ mm}$, $n = 60000 \text{ min}^{-1}$, $a_e = 0.15\text{mm}$ | | | | |

The numerical value of the range R is used to determine the significance sequence of influence factors. By comparing difference ranges of four factors, the significance sequence of four influence parameters for wear band width from large to small is feed per tooth, axial depth of cut, spindle speed and radial depth of cut.

The relationship between the wear band width and various factors is shown in Figure 9. With increasement of the radial depth of cut, the tool wear width first increases and then decreases, and reaches the minimum when $a_e = 0.15$ mm. The width of tool wear first increases and then decreases with the increasement of axial depth of cut, and it presents the minimum when $a_p = 0.3$ mm. With the increasement of feed per tooth, the tool wear width decreases first and then increases, and it reaches the minimum when $f_z = 2$ $\mu\text{m/z}$. When the spindle speed increases, the tool wear width decreases first and then increases, and it reaches the minimum when $n = 60,000$ min^{-1} . It shows that the optimal combination of milling parameters is $a_e = 0.15$ mm, $a_p = 0.3$ mm, $f_z = 2$ $\mu\text{m/z}$ and $n = 60,000$ min^{-1} .

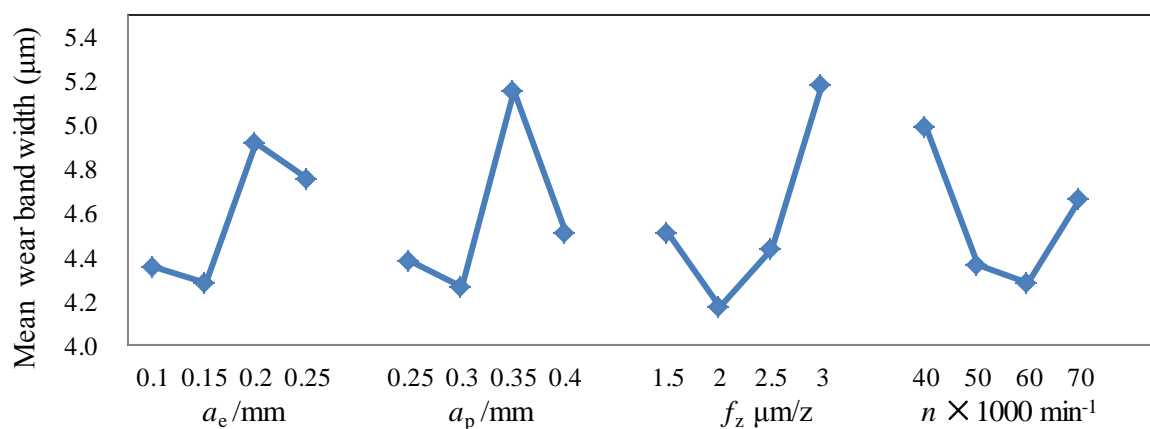


Figure 9. Relationship of wear band width and four factors.

3.3. Optimization parameter validation experiments

In order to verify the correctness of orthogonal optimization experiments, the verification experiments are further carried out by using optimal parameter combination ($f_z = 2$ $\mu\text{m/z}$, $a_p = 0.3$ mm, $n = 60,000$ min^{-1} , $a_e = 0.15$ mm). The workpiece material and micro end tool are consistent with the previous experiments. At the end of the experiments, the wear band width of the tool surface is measured of $L = 1.28$ μm . The wear band width of validation experiment is smaller than the minimum value of that in the orthogonal experiments. It indicates that optimized parameters combination obtained is reasonable.

4. Conclusions

In this paper, the tool wear of side cutting edge in micro-milling has been experimental studied considering key parameters, wear form and wear mechanism. For micro-milling brass H59, the main wear forms of tool wear are coating peeling, the rounding of corner radius and cutting edge chipping. The orthogonal experiments results show that the significance order of key parameters for wear band width of side cutting edge from large to small is feed engagement f_z , axial depth of cut a_p , spindle speed n and radial depth of cut a_e . The optimal parameters combination in the optimization experiment is $f_z = 2$ $\mu\text{m/z}$, $a_p = 0.3$ mm, $n = 60,000$ min^{-1} , $a_e = 0.15$ mm. The width of tool wear is 1.28 μm in optimization verification experiment, and it verifies the correctness of the optimal milling parameters selected in this experiments. The study has significant meaning for reducing the tool wear, improving the tool life, reducing the machining cost and promoting the development of micro milling processing.

Acknowledgement

The authors wish to express their appreciations for the financial support by the Nature Science Foundation of Shandong Province with the grant number of ZR2015EL023, the Nature Science Foundation of China with the grant number of 51505264, and the SDUT & Zibo City Integration Development Project with the grant number of 2017ZBXC189.

References

- [1] Creighton E, Honegger A, Tulsian A, Mukhopadhyay D 2010 Analysis of thermal errors in a high-speed micro-milling spindle. *International Journal of Machine Tools & Manufacture* **50**(4) 386-393
- [2] Malekian M, Park S S, Jun M B G 2009 Tool wear monitoring of micro-milling operations. *Journal of Materials Processing Tech* **209**(10) 4903-14.
- [3] Sredanovic B., Globocki Lakic G, Kramar D, Kopac J 2016 Analysis of micro-milling of hardened tool steel. *Key Engineering Materials* **686** 57-62.
- [4] Kuram E, Ozelik B 2013 Multi-objective optimization using Taguchi based grey relational analysis for micro-milling of Al 7075 material with ball nose end mill. *Measurement* **46**(6) 1849-64.
- [5] Zhu K, Hong G S, San W Y, Multiscale S 2011 Analysis of Cutting Forces for Micromilling Tool-Wear Monitoring. *IEEE Transactions on Industrial Electronics* **58**(6) 2512-21.
- [6] Saedon J B, Soo S L, Aspinwall D K, Barnacle A, Saad N H 2012 Prediction and optimization of tool life in micro-milling AISI D2 (~62 HRC) hardened steel. *Procedia Engineering* **41**(41) 1674-83.
- [7] Biermann, D, Steiner M, et al 2013 Investigation of different hard coatings for micro-milling of austenitic stainless steel. *Proc Forty Sixth CIRP Conference on Manufacturing Systems* (Germany: Procedia Cirp) p246-251.
- [8] Thepsonthi T, Özel T 2014 An integrated toolpath and process parameter optimization for high-performance micro-milling process of Ti-6Al-4V titanium alloy. *International Journal of Advanced Manufacturing Technology* **75**(1-4) 57-75.
- [9] Popov K, Elkaseer A, et al 2010 Material Microstructure Effect-based Investigation of Tool Wear in Micro-endmilling of Multi-phase Materials. *Int Con on Multi-Material MICRO Manufacture* (Monterrey, Mexico: Society of Manufacturing Engineers) p201-08
- [10] Oliaei S N B, Karpas Y 2016 Influence of tool wear on machining forces and tool deflections during micro milling. *International Journal of Advanced Manufacturing Technology* **84**(9-12) 1963-80.
- [11] Cheng X, Li L, Huang, Y, Yang X, Zhou S 2015 Theoretical modeling of the critical conditions for ductile-regime milling of single crystalline silicon. *Journal of Mechanical Engineering Science* **229**(8) 1989-96
- [12] Zhang S, Cheng X, Yang X H, Dai Y J 2014 Development of a desktop ultra-precision micro milling machine. *Machinery Design & Manufacture* **1**(01) 110-2